Modeling Solar Spectral Irradiance under Tropical Atmospheric Conditions

HUAN JIA YAN

A0083300X

SUPERVISOR: DR. LIEW SOO CHIN

A Thesis submitted in partial fulfilment for the degree of Bachelor of Science (Honours) in Physics

Acknowledgment

I would like to thank Dr Liew Soo Chin for his guidance and patience over the past year. I have learnt a lot from his teaching and about research work. I would also like to thank Dr Santo V. Salinas Cortijo and Dr Chang Chew Wei for their assistance.

Lastly I would like to thank my friends and family for the care and help for this thesis.

Abstract

Measurements of solar spectral irradiance were collected over the period of October 2014 to January 2015, in order to investigate the compatibility of the SMARTS irradiance model to model solar spectral irradiance under the tropical atmospheric conditions in Singapore. By modifying SMARTS2 Radiative Transfer Model, this project also aims to create an empirical model to predict solar irradiance accurately in Singapore.

Contents

List of Figures

1. Introduction

1.1 Solar Irradiance and Irradiance Models

Solar Irradiance refers to the incoming radiant flux per unit area incident on the Earth's surface produced by the Sun in the form of electromagnetic radiation. As incoming sun radiation is the greatest and most vital source of energy supply to the Earth's system, it is of great importance and usefulness to understand and model the solar irradiance we receive.

The atmosphere plays a very important role in determining the total amount of solar irradiance received on the Earth's surface, as it results in the attenuation of incoming solar radiation through scattering and absorption processes. The above phenomena is known as radiative transfer in scientific studies. As the atmosphere is a very dynamic system which varies with altitude and geographical location, a rigorous model is needed to provide a reasonable estimate of the solar irradiance spectrum.

Till date, there have been many spectral irradiance models developed, each adopting a different approach to understand and compute the amount solar radiation transmitted through the atmosphere. Basic analytical models are based on the theory of radiative transfer and solved under simplified assumptions. More rigorous and practical models are similarly based the theory of radiative transfer. However, they depend on numerical methods and rigorous codes to solve the equation of radiative transfer at different layers of the atmosphere. One famous examples is MODTRAN (MODerate resolution atmospheric TRANsmission), an atmospheric code written by US Air Force Phillips Laboratory. Some other radiative transfer code are based parameterisation of spectral transmittance functions of main extinction processes in the atmosphere. SMARTS or the Simple Model of Atmospheric Radiative

Transfer (Gueymard 1995), which we would be studying in this paper, is an example of such models.

Models mentioned above are clear sky models. Certain empirical models attempts to take into account the effect of clouds. These models, are known as sky radiance models where it models the radiance coming from each sky patch and integrates over the entire sky dome to obtain total irradiance.

A great number of applications, such as agriculture, remote sensing, oceanic studies, climatic studies and solar energy harvesting industries require a reasonable prediction of solar irradiance as ability and practicability of actual measurements may not always be a possible. For instance, being able to estimate the amount of solar irradiance incident on the ocean surface can allow one to understand the optical properties of the ocean water, its depth and also estimates its temperature. This knowledge are important for climatic studies as the ocean waters have huge impact on extreme weather in coastal areas and thermal expansion of seawater. Moreover, certain remote areas of the ocean are not accessible for actual measurement. These reasons, hence, motivates the development of spectral irradiance models.

In this paper, we attempt to modify the SMARTS spectrum to describe local solar spectral irradiance through empirical methods. The tropical region which Singapore is located at is characterised by warm, humid and cloudy atmosphere. In particular, the humidity and cloudiness directly affect the solar irradiance we receive at Earth's surface.

This paper introduces the basic theory behind (i) interaction between insolation and the atmosphere and (ii) the modelling of solar spectral irradiance. It will then discuss in greater depth the compatibility of such models with local conditions and possible corrections that can be applied to the model.

1.2 Objective

The main purpose of this thesis is to investigate the suitability of "Simple Model of Atmospheric Radiative Transfer of Sunshine (SMARTS)" to model Singapore's solar spectral irradiance. The research was carried out in two major parts as listed below.

1. Investigate compatibility of computational solar irradiance model SMARTS to predict Singapore's solar irradiance spectrum using AERONET data.

2. Empirical correction of SMARTS-generated solar irradiance spectrum to account for discrepancies with measured irradiance and understanding the variation of correction parameters under different atmospheric conditions

2. Theory

2.1 Solar Irradiance

The solar irradiance spectrum is defined as the spectral distributions of incident solar flux on the surface of the Earth. It typically spans the ultraviolet region, visible region to the near infrared, and peaks about the visible region.

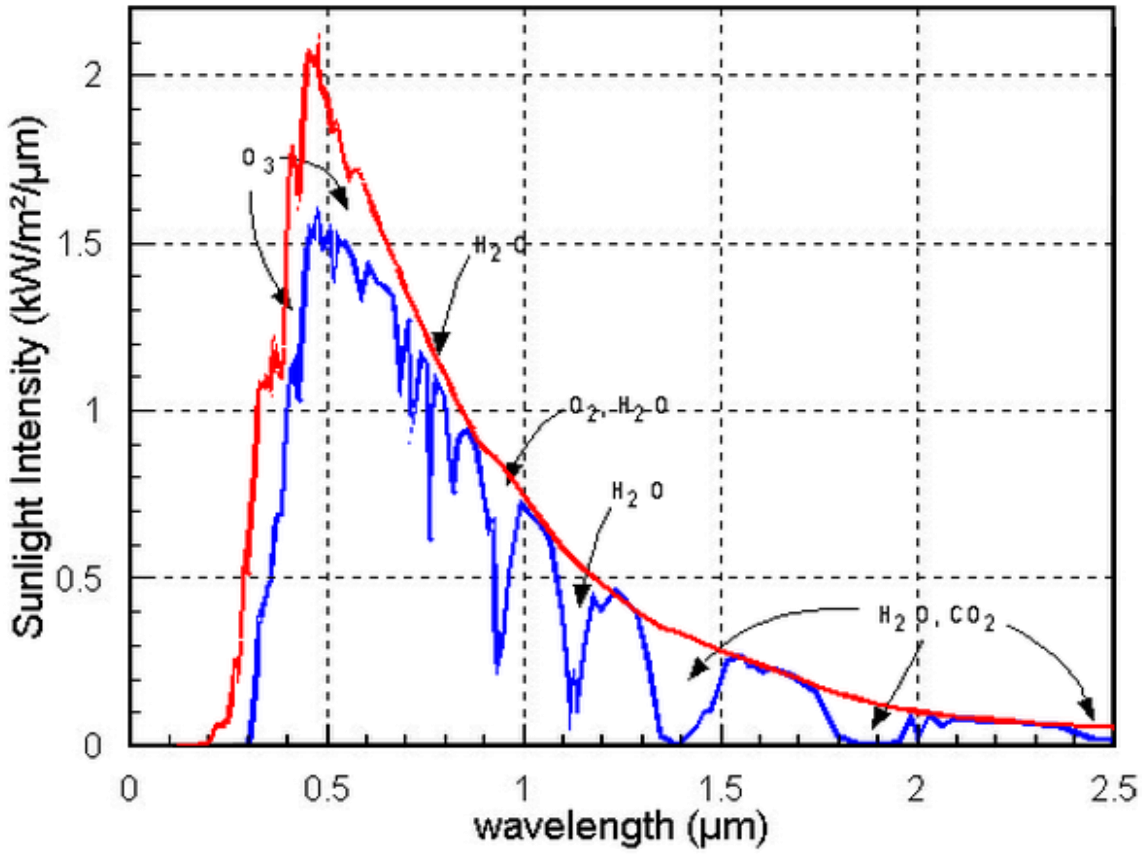

Figure 1 AM0 Solar Irradiance Spectrum in comparison with AM1.5 Solar Irradiance Spectrum. AM stands for Air Mass, where AM0 refers to the top of atmosphere and AM1.5 refers to an air mass 1.5 times that of the vertical height of the atmosphere.

The global (total) irradiance receive at the Earth's surface is usually separated into two components: the direct and diffuse irradiance. The direct irradiance refers to the attenuated

beam of direct sunlight which reaches the Earth's surface as it travels through the atmosphere. The diffuse irradiance component on the other hand, refers to photons scattered away from the direct beam that eventually reaches the Earth's surface through multiple scattering. The diffuse radiance comes from all the directions of the sky. Another main feature of the solar irradiance spectrum are absorption bands due to absorption by various chemical species in the atmosphere, such as carbon dioxide and water vapour.

2.2 Atmosphere

2.2.1 Radiative Transfer Equation

The equation of radiative transfer describes the interaction of electromagnetic radiation (energy transfer) as it propagates through a medium. It is widely used to describe and understand the atmospheric radiative transfer of solar radiation. As solar radiation propagates through the atmosphere, it experiences absorption, emission and scattering.

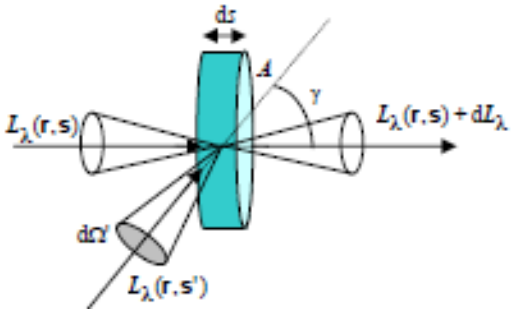

Figure 2

Considering a radiance L_λ propagating through a medium *ds* as shown in figure 2, we can compute the radiance change by considering the following three components.

i. Extinction of Direct Beam

The extinction of direct beam, which includes both absorption and scattering, is modelled by the Beer–Lambert–Bouguer law in equation (1) below where β_e denotes the extinction coefficient.

$$dL_\lambda = -L_\lambda(r,s)\beta_e(r;\lambda)ds \tag{1}$$

ii. Scattering of flux

Another main component contributing to radiance is due to scattering of flux, coming from all other directions. The increase in flux due to scattering can be described by the following equation.

$$dL_{\lambda,scattered} = \frac{\omega(r,\lambda)\beta_e(r;\lambda)ds}{4\pi}\int P(s,s';r,\lambda)L_\lambda(r,s')d\Omega \tag{2}$$

Here, ω refers to the single scattering albedo, defined at the ratio of scattering cross-section to extinction cross-section; P is the scattering phase function.

iii. Thermal Emission

Lastly, thermal emission also makes an important contribution to the change in radiative transfer. A scattering volume at a temperature *T* emits blackbody radiation according to the Planck Law, resulting to an increase in the radiance along the direction s, where $B_\lambda(T)$ is the blackbody radiance.

$$dL_{\lambda,\text{emission}}(r,s) = [1 - \omega(r,\lambda)]\,\beta_e(r;\lambda)\,B_\lambda(T(r))ds \quad (3)$$

Hence these components combine to give the Radiative Transfer Equation (RTE).

$$dL_\lambda = dL_{\lambda,direct} + dL_{\lambda,scatter} + dL_{\lambda,thermal} \quad (4)$$

Equation (4) simplifies to (5), where $J_{\lambda,scattered}$ and $J_{\lambda,emission}$ are defined as follows.

$$\frac{1}{\beta_e(r,\lambda)}(s\cdot\nabla)L_\lambda(r,s) = -L_\lambda(r,s) + J_{\lambda,scattering}(r,s) + J_{\lambda,emission}(r,s) \quad (5)$$

$$J_{\lambda,scattered} = \frac{\omega(r,\lambda)}{4\pi}\int p(s,s';r,\lambda)L_\lambda(r,s')d\Omega \quad (6)$$

$$J_{\lambda,\text{emission}}(r,s) = [1 - \omega(r,\lambda)]\,B_\lambda(T(r)) \quad (7)$$

To solve the RTE is non-trivial. Moreover, atmospheric properties varies with altitude. It is usually not possible to obtain the solution in a simple analytical function. A common approach is to apply numerical computational methods to solve the RTE and compute the solar irradiance under specific circumstances. Important information required to solve the RTE includes the atmospheric constituents, aerosol models and optical thicknesses.

2.2.2 Aerosol

Aerosols are particulate matter suspended in the air which interacts with insolation through scattering and absorption. Aerosols vary greatly in concentration, size, composition and consequently their optical effects. Their effects also vary at different layers of atmosphere. The effect of aerosol manifest in the value of the single scattering albedo, the asymmetric factor as well as the angstrom component and consequently the aerosol optical depth (or

aerosol optical thickness). The aerosol optical depth, τ_a, is the degree to which aerosols prevent the transmission of light by absorption or scattering of light. It is a wavelength dependent property as in equation (7), modified by the angstrom exponent α which is dependent on aerosol properties.

$$\tau_a(\lambda) = \tau_a(\lambda_{ref})\left(\frac{\lambda_{ref}}{\lambda}\right)^{\alpha} \quad (7)$$

Over the years, many aerosol models, (such as *Shettle & Fenn, 1979*) have been developed to simulate the aerosol type and distribution for different atmospheric conditions (e.g. urban, maritime and rural). These models are often used by radiative transfer models to compute the effects of aerosol in atmospheric transmittance and scattering distribution of sunlight. Aerosol models first attempts to determine the size distribution and refractive index aerosol particles under certain environmental conditions and then proceed with Mie Scattering calculation to obtain extinction (scattering and absorption) coefficients from which single scattering albedo ω, asymmetry g and the scattering phase function can be obtained. (*Shettle, E. P., & Fenn, R. W., 1979)*

2.2.3 Clouds

A component often excluded in the RTE models is the factor of clouds. This is due to the high variability of cloud cover which renders it hard to model. Clouds differ in type, size, height and temperature and thus interfere with the insolation differently.

Due to the high albedo of clouds, it reflects incoming shortwave radiation. In particular, low and thick clouds reduces the incoming shortwave radiation. On the other hand, high and thin

clouds are mostly transparent to incoming shortwave radiation. They absorb and re-emit longwave radiation, and hence act like clean air.

While clouds have a significant influence on the solar irradiance attenuation, spectral effects of clouds are poorly known (Bartlett 1998). In the later part of this paper, we attempt at studying the effects of clouds on the solar irradiance through our experimental observations.

2.3 Solar Irradiance Models

Hitherto, many spectral solar irradiance models has been developed. These models varies from rigorous numerical codes, parameterised functions to empirical models. Rigorous code such as MODTRAN simulates the atmosphere using thirty-three distinctive layers with atmospheric parameters such as temperature, pressure and extinction coefficients defined for each layer and uses numerical methods to calculate diffuse irradiance. (*Gueymard 2004*) Other scientific and engineering models such as Simple Model of Atmospheric Radiative Transfer of Sunshine (SMARTS) and SPCTRAL rely on parameterization of various transmittance functions, working based on MODTRAN codes with a more user friendly interface.

In this paper, the applicability of SMARTS computational code to model Singapore's solar irradiance is being studied. Due to Singapore's geographical location, the sky is often cloudy. Hence, it is interesting and important to study the compatibility of the clear sky model with Singapore's weather.

Let us first consider an analytical model to better understand the radiative transfer of solar irradiance.

2.3.1 Analytical Model

We now attempt to obtain an irradiance spectrum by solving the radiative transfer equation using single scattering approximation, that is incoming photons only experience scattering at most once before reaching the Earth's surface.

$$E_{\lambda}^{\downarrow} = E_{\lambda,dir}^{\downarrow} + E_{\lambda,dif}^{\downarrow} \tag{8}$$

As shown in (8), the downwards irradiance $E_{\lambda}^{\downarrow}$ can be divided into two components, the direct and diffuse component. The equation (8) can also be rewritten in the form as seen in (9) where $T^{\downarrow}_{\lambda,dir}$ and $T^{\downarrow}_{\lambda,dif}$ are direct and diffuse downward transmittance.

$$E_{\lambda}^{\downarrow} = F_{\lambda} u_s (T_{\lambda,dir}^{\downarrow} + T_{\lambda,dif}^{\downarrow}) \tag{9}$$

$$T_{\lambda,dir}^{\downarrow} = \exp\left(\frac{\tau}{u_s}\right) \tag{10}$$

$$T_{\lambda,dif}^{\downarrow} = \frac{\omega}{4\pi} \int_0^{2\pi} \int_{-1}^{0} \left(\frac{|u|}{|u| - u_s}\right) \left(\exp\left(-\frac{\tau}{|u|}\right) - \exp\left(-\frac{\tau}{u_s}\right)\right) P(u; u_s) du d\phi \tag{11}$$

Suppose the atmosphere is divided into two non-mixing layers, one consisting of only aerosols, and the other, molecules. The equation (9) would be become (12), where the total transmittance ($T^{\downarrow}_{\lambda,dir} + T^{\downarrow}_{\lambda,dif}$) is calculated for each layer of atmosphere.

$$E_{\lambda}^{\downarrow} = F_{\lambda} u_s (T_a^{\downarrow} \cdot T_r^{\downarrow}) \tag{12}$$

T_a and T_r refers to total transmittance through the aerosol and molecule layer respectively.

In the molecular layer, scattering is modelled by Rayleigh scattering, whose aerosol optical depth τ_r and phase function $P(\gamma)$ are shown in (13) and (16) respectively. A phase function value at a certain scattering angle γ gives the probability of an incident photon scattering in that direction.

$$\tau_r = \frac{a_1}{\lambda^4}\left(1+\frac{a_2}{\lambda^2}+\frac{a_3}{\lambda^4}\right) \tag{13}$$

$$P = \frac{3}{4}\left(1+\cos^2\gamma\right) \tag{14}$$

Under standard atmospheric pressure and temperature, the values of the coefficient in (15) are

$$a_1 = 0.008569\mu m^4; a_2 = 0.0113\mu m^2; a_3 = 0.00013\mu m^4 \tag{15}$$

In the aerosol layer, suppose we model the phase function $P(\gamma)$ by equation (16),

$$P(\gamma) = a + b\delta(\cos\gamma - 1) \tag{16}$$

From the following relationship between the phase function and its asymmetricity[1] g (equation (17)) we can rewrite (16) in terms of its asymmetricity (18).

$$g = \frac{\int_0^{2\pi}\int_0^{\pi} P(\gamma)\cos\gamma\sin\gamma d\gamma d\phi}{\int_0^{2\pi}\int_0^{\pi} P(\gamma)\cos\gamma\sin\gamma d\gamma} \tag{17}$$

[1] Asymmetricity is defined as the mean value of the cosine of scattering angle γ of a phase function

$$P(\gamma) = 1 - g + 2g\delta(\cos\gamma - 1) \tag{18}$$

Values of g and τ_a were calculated using solar irradiance computation model and substituted into the respective equations. With the assumption that the Rayleigh and aerosol optical thicknesses were small, equation (12) is evaluated to be

$$E_\lambda = F_\lambda u_s \left(e^{-\frac{\tau_a}{u_s}} + \frac{(1-g)\omega\tau_a}{2u_s} + \frac{\omega g \tau_a}{u_s}(\phi_s - \pi) e^{-\frac{\tau_a}{u_s}} \right) \left(e^{-\frac{\tau_r}{u_s}} + \frac{\omega\tau_r}{2u_s} \right) \tag{19}$$

which gives us the expression for irradiance under single scattering approximation.

Figure 3 to 6 below compares the simple single-scattering analytical model to a more rigorous atmospheric transfer code SMARTS, using the same input parameters. The input parameters (single scattering albedo ω, aerosol optical depth τ_a and asymmetricity g) are derived from SMARTS using maritime and aerosol models respectively. Results shows that the analytical predicts a spectrum of a similar shape, or rather, spectral distribution as the SMARTS models. However, it does not calculate the absorption bands. Furthermore, the two models differs greatly at higher aerosol optical depth (AOD or τ_a). This is so as one would expect multiple scattering at higher AOD as oppose to single scattering.

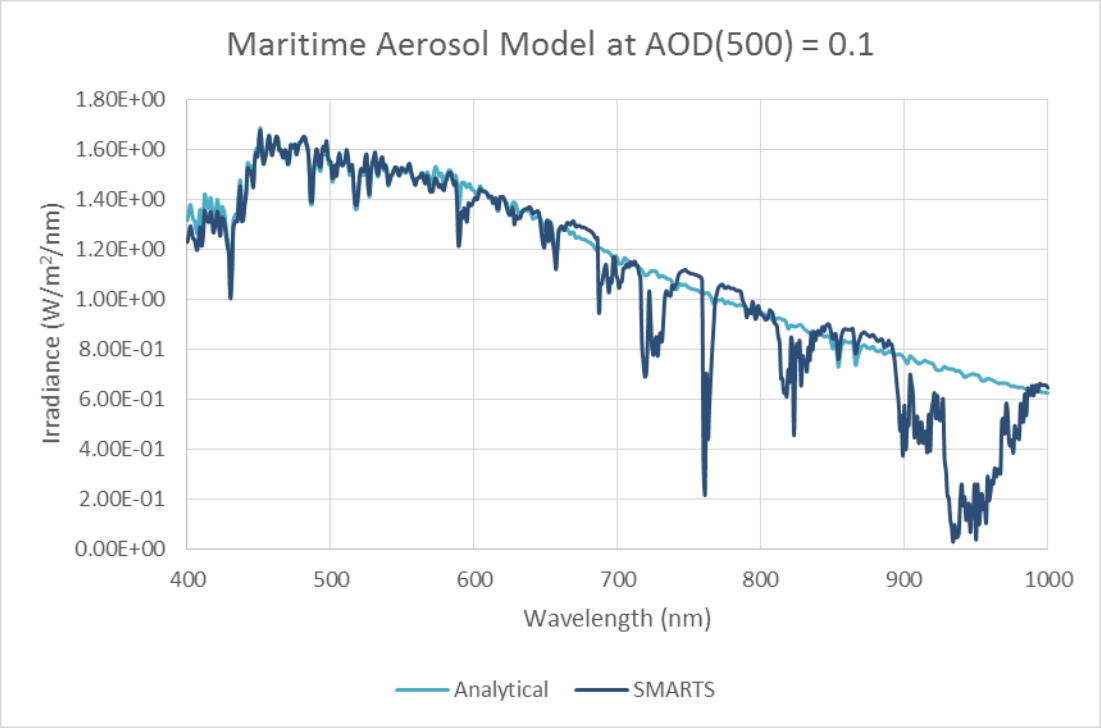

Figure 3 Analytical Model Irradiance vs. SMARTS-generated Irradiance based on Maritime Aerosol Model at AOD = 0.1

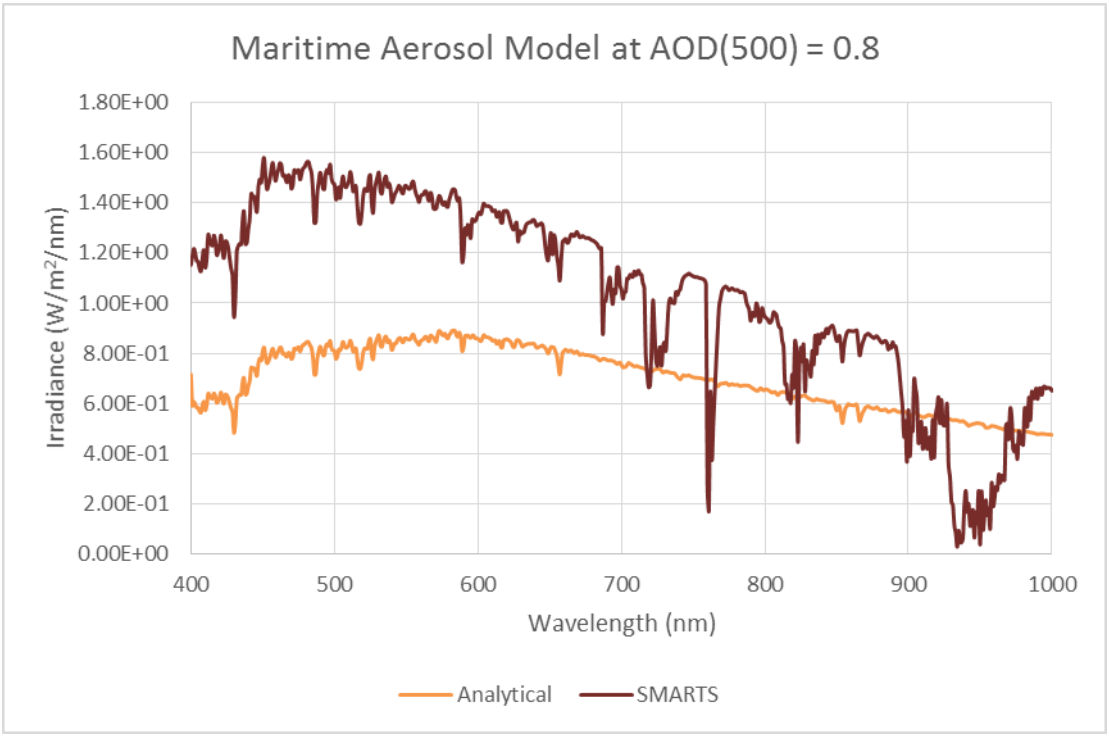

Figure 4 Analytical Model Irradiance vs. SMARTS-generated Irradiance based on Maritime Aerosol Model at AOD = 0.8

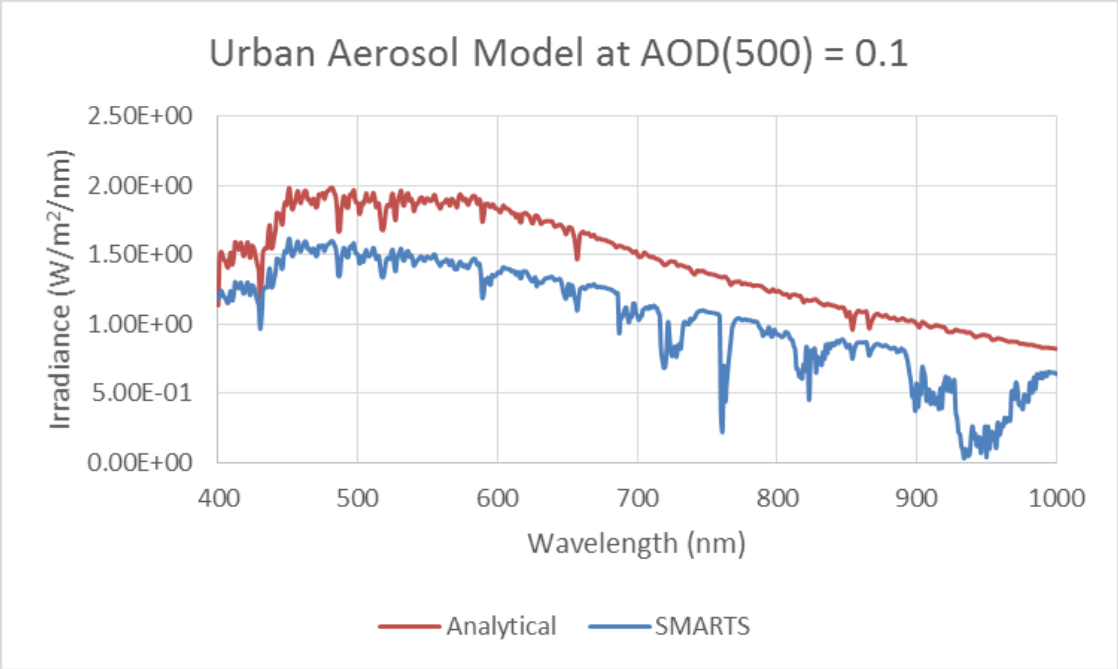

Figure 5 Analytical Model Irradiance vs. SMARTS-generated Irradiance based on Urban Aerosol Model at AOD = 0.1

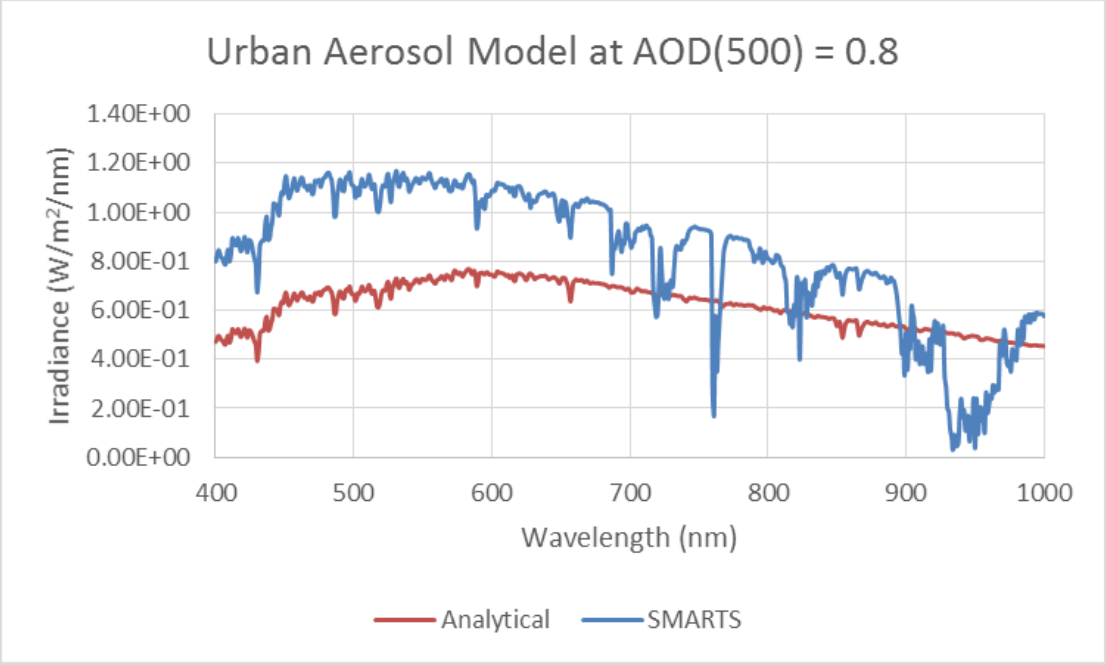

Figure 6 Analytical Model Irradiance vs. SMARTS-generated Irradiance based on Urban Aerosol Model at AOD = 0.8

2.3.2 Modelling basis of SMARTS V2.9.5

The Simple Model of the Atmospheric Radiative Transfer of Sunshine (SMARTS) is a spectral irradiance model. It uses FORTRAN code to predict the direct beam, diffuse, and global irradiance incident on the Earth's surface. The model covers the entire shortwave solar spectrum (280 to 4000 nm), including the UVA, UVB, Visible and Near-Infrared bands.

The following section is a brief description on the principles of SMARTS (*Gueymard, 2001*)

(a) Direct Beam Irradiance

The solar shortwave direct beam irradiance, $E_{bn\lambda}$, is calculated from spectral transmittance functions for main extinction processes in a cloudless atmosphere. These extinction processes include Rayleigh scattering, ozone extinction, nitrogen dioxide extinction, mixed gases extinction, water vapour extinction and aerosol extinction and are represented by their respective transmittance functions T in equation (20).

$$E_{bn\lambda} = E_{on\lambda} T_{R\lambda} T_{o\lambda} T_{n\lambda} T_{g\lambda} T_{w\lambda} T_{a\lambda} \tag{20}$$

$E_{on\lambda}$ in equation (20) is the extra-terrestrial irradiance corrected for actual Earth-Sun system. The general form of the various transmittance functions T are modelled by the Beer–Lambert–Bouguer law as seen in (1). The optical depth of respective transmittance function of various chemical species can be provided by users, or otherwise estimated from standard atmospheres provided by SMARTS. As there is a lack of detailed aerosol data, SMARTS adopts modified two-tier Ångström approach (Bird, 1940) to determine aerosol optical depth. The approach considers two spectral regions, above and below λ_0 = 500nm. The aerosol optical depth at 500nm is supplied by the user.

(b) Diffused Irradiance

SMARTS adopts a simplified approach to calculate the diffused irradiance by using the same transmittance functions used to calculate the direct beam irradiance. (Gueymard, 1995) It is based on the idea that any photon from the direct beam that was not transmitted are being scattered in all directions. Hence the model predicts the diffused downward irradiance by taking a proportion of these scattered photons. This fraction is determined by studying the three components which sums up to the total diffused irradiance – Rayleigh scattering, aerosol scattering, ground and sky backscattering. Multiple scattering is also taken into account by this approach.

The global irradiance is found by adding the direct and diffused irradiance.

(c) Aerosol models

As demonstrated above in figures 3 to 6, aerosol models affects the spectral distribution of solar irradiance. Scattering functions require information on the single scattering albedo ω and asymmetry g. These values are calculated from aerosol models used in the computation of irradiance. SMARTS allows the user to choose from various aerosol models, such as the Shettle and Fenn (S&F) model, Standard Reference Aerosol (SRA) model and Braslau & Dave model. User defined models is also an available option.

2.3.3 Optical Properties of Atmospheric Parameters

In order to facilitate our understanding of the role each parameters in SMARTS computation. This section serves to demonstrate the effect of the precipitable water, aerosol optical depth at 500nm and aerosol model. This understanding is important to help us evaluate the compatibility of SMARTS to predict local spectral irradiance.

(a) Precipitable Water

Precipitable water is defined to be the height, in centimetres, of a column of liquid water with cross-section of 1cm^2, that would be formed, supposing that all the water vapour in the zenith direction from ground up is condensed. (*Gueymard and Kambezidis, 2004*). The amount of precipitable water determines the depth of the water absorption bands. Within the range of our research interest, the absorption bands are found at 720nm, 820nm and 940nm.

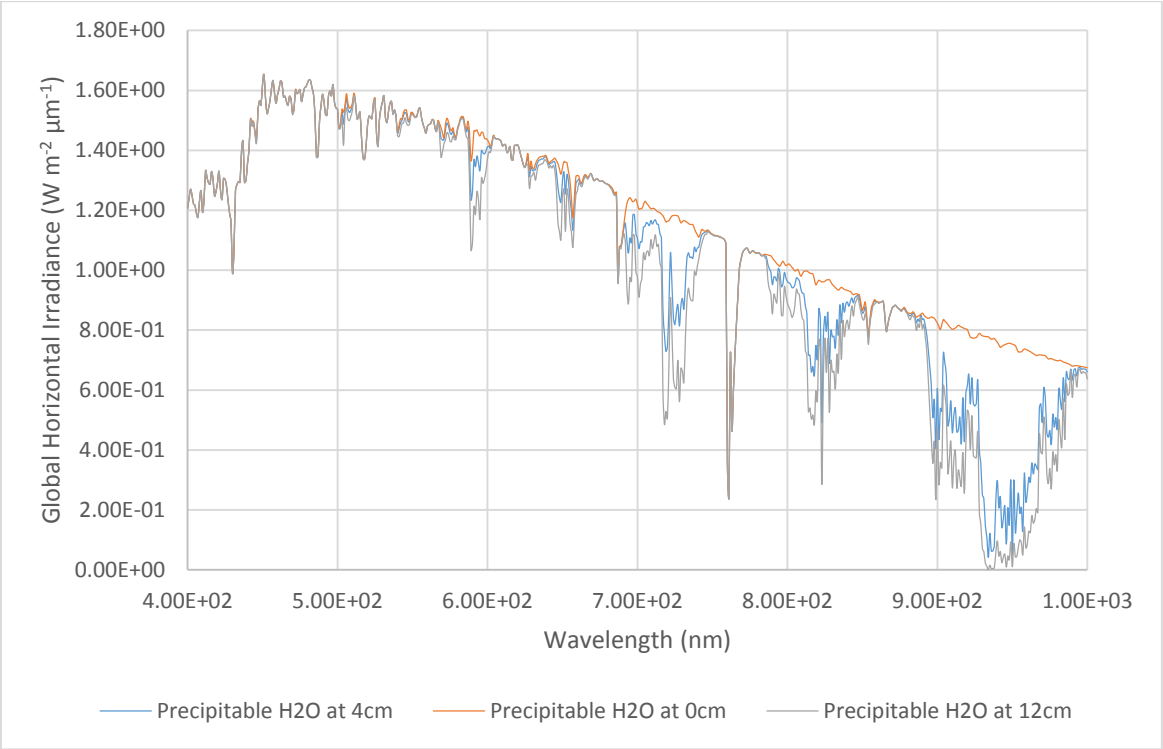

Figure 7 Global Horizontal Irradiance for different values of precipitable water

As seen in figure 7, with increasing precipitable water, the depth at the water vapour absorption bands increases. This high humidity is a signature of tropical climate, accurate prediction of water vapour absorption is important.

(b) Aerosol Optical Depth, τ_a

As defined in the earlier section, aerosol optical depth (AOD or τ_a) is the degree to which aerosols prevent the transmission of light by absorption or scattering of light. It is a very important parameter in understanding the transmittance of solar radiation. Changes in the AOD affects both the height and spectral distribution of the irradiance as shown in figure 8. This is due to the change in absorption and scattering processes as AOD changes.

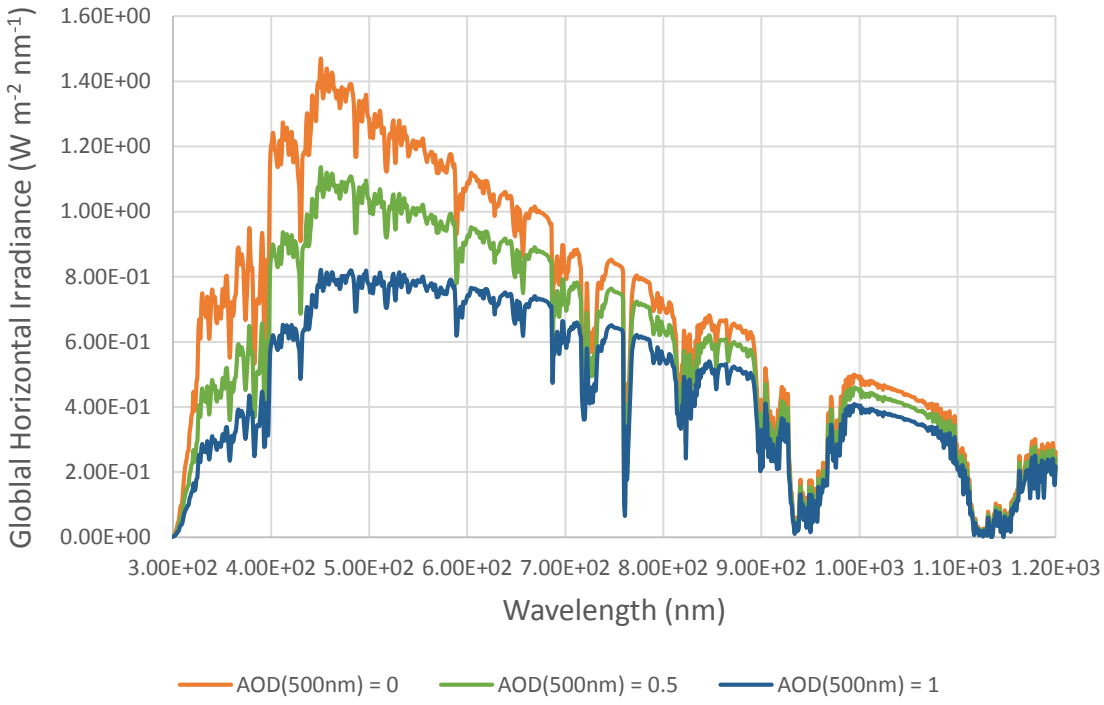

Figure 8 Global Horizontal Irradiance for different values of AOD

(c) Aerosol Models

Choosing a suitable aerosol model is important to obtain a good prediction of the solar spectral irradiance, given the above parameters.

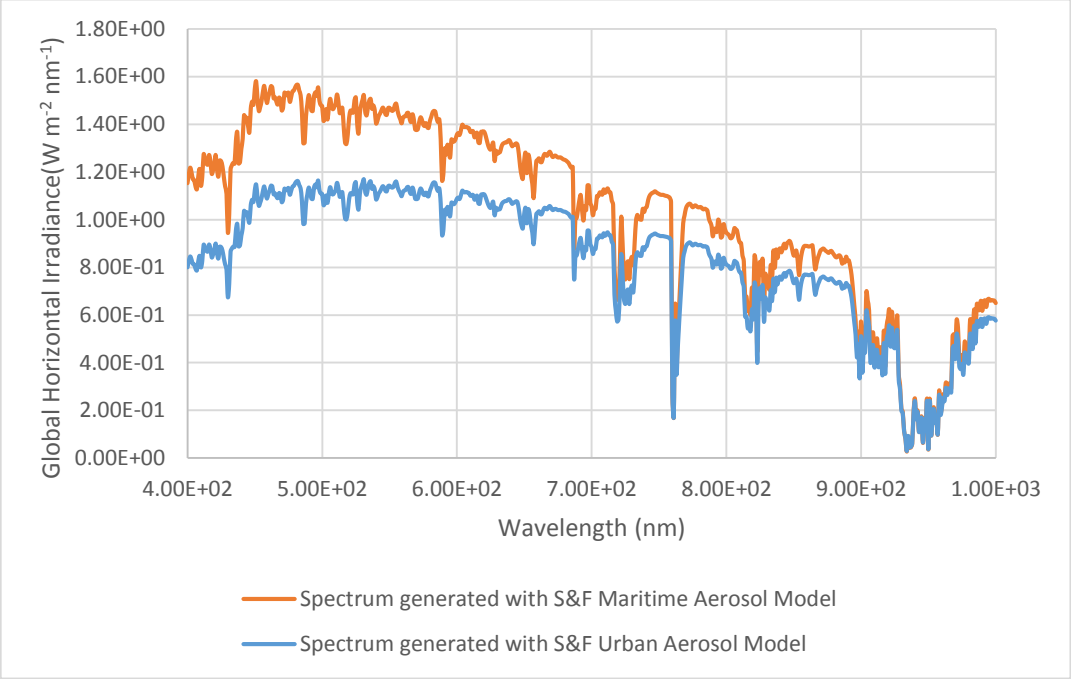

Figure 9 Global Horizontal Irradiance under same atmospheric conditions with different aerosol models

As shown in figure 9, while using the same parameters, different aerosol models predicts a different irradiance spectrum. This is because different aerosol models adopt different size distribution and hence calculates different asymmetricity and single scattering albedo. This in turn alters the diffuse component of the spectrum and generates a different global irradiance spectrum.

To demonstrate this, we alter aerosol optical depth input into to both the maritime and urban aerosol model and compare their direct and diffuse components. Figure 10(a)(i) and (a)(ii) compares the two spectrums modelled with urban aerosol model while figure 10(b)(i) and (b)(ii) compares the spectrums modelled with maritime aerosol model. At small AOD, the difference between urban and maritime aerosol

model is not obvious. However, comparing figure 10 (a)(ii) and (b)(ii), where AOD was larger, the spectral distribution of the direct and diffuse spectrum predicted by the two models is drastically different. Thus one could clearly perceive the difference aerosol models can cause to the irradiance calculations.

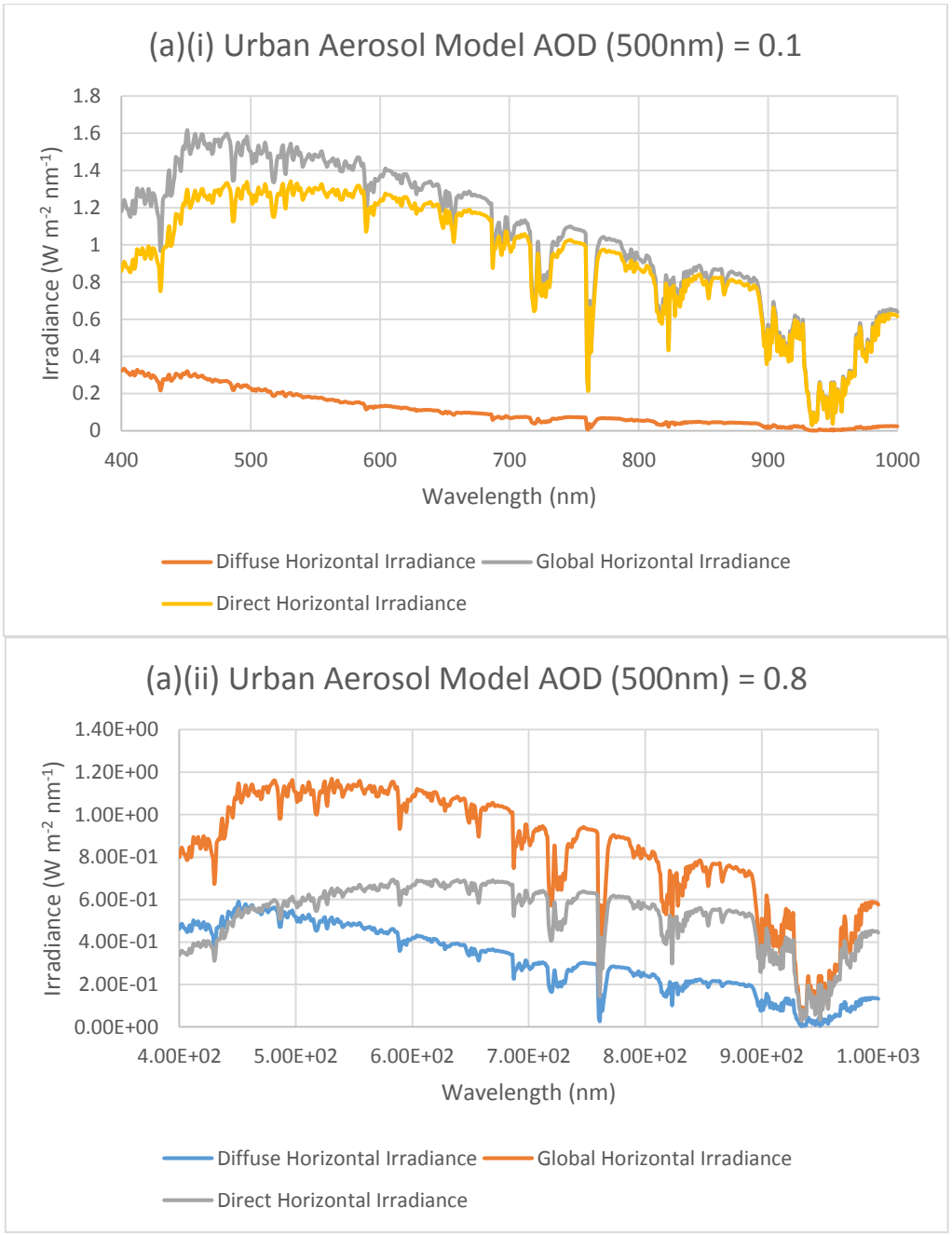

Figure 10 (a) Global, Direct and Diffused Irradiance Spectrum generated using S&F Urban Aerosol Model for (i) AOD(500nm) = 0.1 (ii) AOD(500nm) = 0.8

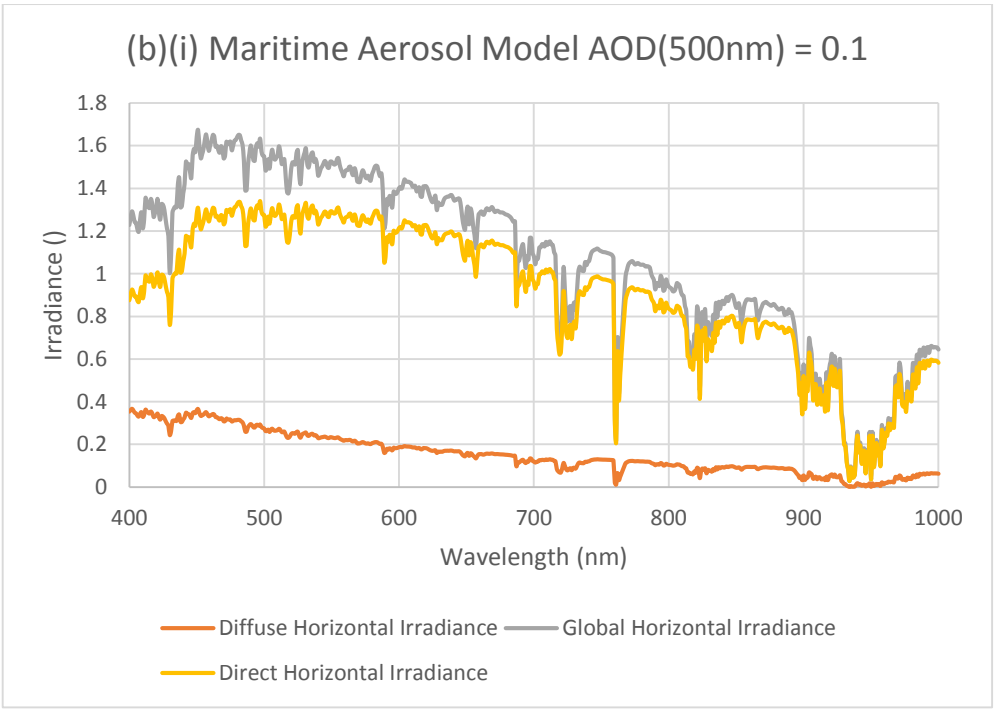

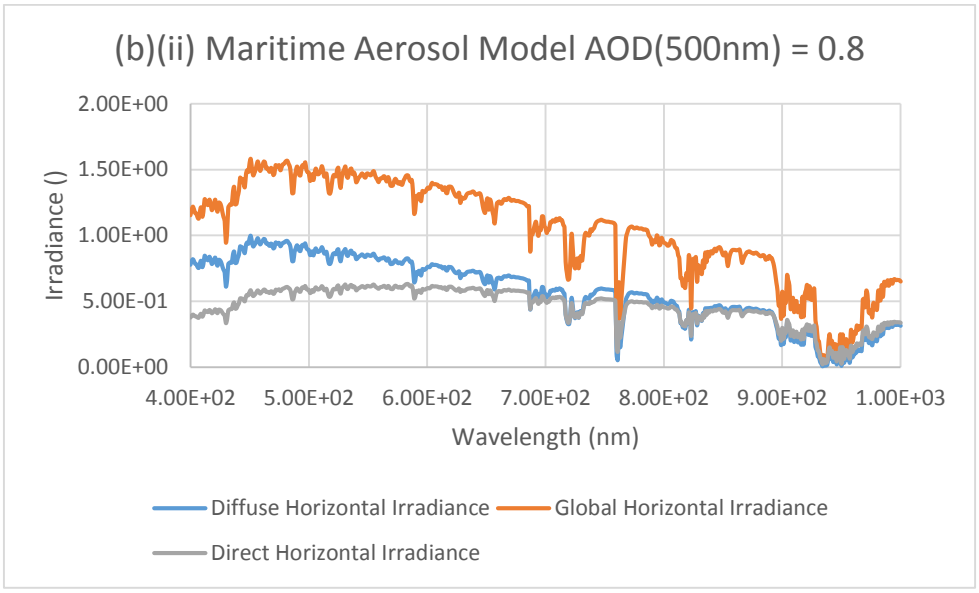

Figure 10 (b) Global, Direct and Diffused Irradiance Spectrum generated using S&F Maritime Aerosol Model

for (i) AOD(500nm) = 0.1 (ii) AOD(500nm) = 0.8

3. Methodology

3.1 Measurements

Measurements of solar irradiance were taken during the period of October 2014 to January 2015 at the Multi-Purpose Field of the National University of Singapore. The multi-purpose field was an open field where there is a considerably clear view of the sky dome. Moreover, it is located near the storage of the equipment and hence, was an ideal site for field measurements. Measurements were usually taken around noon where irradiance was the strongest.

3.1.1 Measurement of Solar Radiance

The Solar Radiance measurement is made using a spectroradiometer and Lambertian reflecting white board as shown below.

Figure 11 GER1500 Spectroradiometer and Lambertian Reflecting Board

The GER1500 is a portable field spectroradiometer, specified to be sensitive to region of 350nm to 1500nm. It consist of a diffraction grating with a silicon diode array. The silicon array has 512 discrete detectors, and hence reads 512 spectral bands. The spectrometer is capable of storing 483 data, which can be downloaded to a computer at a later time. In this experiment, we are concern with the region 400nm to 1000nm as the equipment displays inaccuracy beyond this range.

The white board as shown in above image, has a Lambertian surface, meaning that any light which falls on it, regardless of direction of incidence, will ideally be reflected uniformly in all directions. In addition, the white board would ideally reflect all wavelengths, with a reflectance of close to 1. Hence, by measuring the solar radiance reflected off the Lambertian white board and integrating the radiance value over all directions, the total down welling horizontal solar irradiance (it would hereon be referred to as global horizontal irradiance[2]) was measured.

In order to measure the diffused component, a shading disk is used to block out the Sun, such that only diffused sky radiance falls on the Lambertian white board. At the time of measurement, the shading disk was placed in the direction of the sun. The white board is completely cast in shadows when measurement is taken. Due to the lack of proper equipment, the accuracy of the diffuse measurement may have been compromised. In order to be able to compare the global and diffused component of solar irradiance under the same sky condition, total and diffused radiance measurements were made in quick succession. The direct component is computed subsequently by subtracting the diffused irradiance from the global irradiance.

[2] Horizontal Irradiance refers to the irradiance measured on a horizontal surface

3.1.2 Recording of Cloud Distribution

The sky condition at the time where each radiance measurement was taken was recorded in the form of hemispherical photograph, captured using a wide angle fisheye lens (figure below). The photograph was taken at nearly the same time as the measurement was taken. These photographs were further analysed to calculate the percentage of area of the sky dome occupied by clouds at the time of measurement as well as to record the cloud type.

Figure 12 Nikon D60 4.5mm EX Sigma Fish-eye lens with 180 °angle of view

Figure 13 Hemispherical Photograph of the sky dome

3.2 Data Processing

3.2.1 Solar Radiance Data

There are two main steps involved in the processing of the raw data of solar radiance.

Firstly, the reflected radiance L measurement had to be integrated over all directions in order to obtain the total irradiance E incident on the Lambertian reflecting white board. As the Lambertian property is such that the reflection of the incident solar radiance isotropic, the integration simplifies to the equation below,

$$E = \pi L \tag{21}$$

Secondly, the 512 spectral bands are not evenly distributed in terms of wavelength interval. Hence, in order to be able to systemically compare the measurements to the computed data by

SMARTS, the raw measurements had to be interpolated. The measurements were interpolated using the cubic spline function.

3.2.2 Hemispherical photographs

The hemispherical photo has a 180 ° field of view which captures the entire sky hemisphere. However, it is geometrically distorted. In order to calculate the percentage of the sky area covered by the clouds (hereon, cloud percentage, k) from the photograph, measurements has to be geometrically corrected. (Schwalbe, 2005)

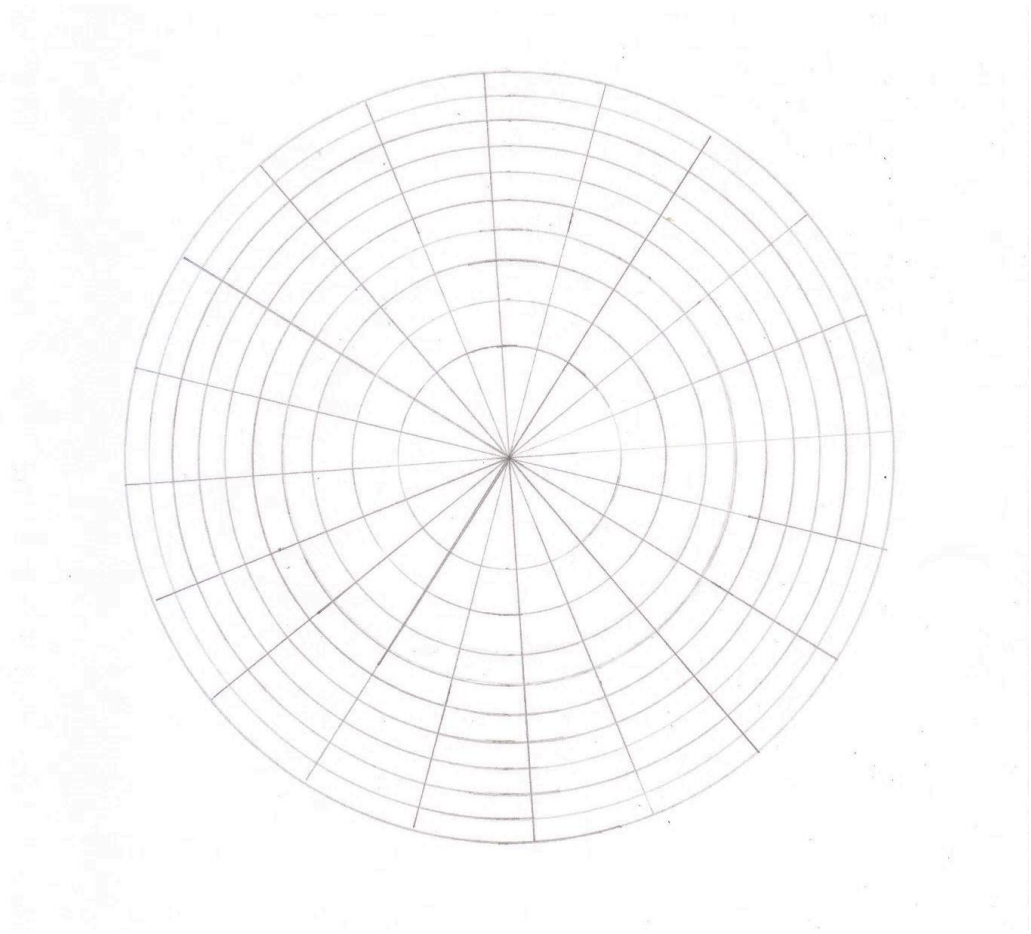

Figure 14

Figure 14 shows the calibrated distribution of area of the sky dome as reflected on the photograph. Each grid corresponds to 0.5 % of the area of the sky dome. By applying this calibration, the cloud percentage, k can be measured.

3.3 Generation of corresponding SMARTS irradiance (based only on AERONET)

Corresponding to each set of field measurement, a SMART irradiance spectrum is generated. This SMARTS spectrum is generated based on the atmospheric condition at the time of the field measurement. Information on the atmospheric conditions are retrieved from the AERONET database.

3.3.1 AERONET Data

AERONET (AErosol RObotic NETwork) program is a worldwide network of sun photometers established by NASA for the study of aerosol properties. In Singapore, the sun photometer operates at CRISP building in the National University of Singapore, led by principal investigators Dr Liew Soo Chin and Dr Santo V. Salinas Cortijo. The database containing daily records of AOD, precipitable water, pressure of Singapore.

For input into the SMARTS model, the AERONET data recorded at time that best corresponds to the time of field measurement was chosen.

In our experiment, tropical reference atmosphere is used. Concentration of carbon dioxide CO_2 is obtained from the value measured that the Mauna Loa Observatory. The total precipitable water H_2O, aerosol optical depth τ_a at 500 nm and air pressure are obtained from the AERONET data. Remaining atmospheric content are estimated by SMARTS from the

reference atmosphere. As information on the single scattering albedo ω and asymmetry g are not always available from AERONET, they had to be estimated from aerosol models available for users to choose in the SMARTS model.

The Shettle & Fenn (S&F) aerosol model is chosen as it is humidity-dependent aerosol model (*Shettle & Fenn 1979*), unlike the other options. (*Gueymard 1995*) It is thus suitable for tropical climate modelling. Since the site of measurement would potentially fit into both urban and maritime models, a spectrum is generated for each of these two models using the same input parameters. The SMARTS irradiance model computed from these data is then compared directly with its corresponding measured irradiance spectrum. Upon further analysis, the more suitable aerosol model would be picked.

3.4 Empirical Fitting

Based on the analysis on the comparison between the computed spectrums, we would attempt to minimise discrepancies through empirical correction.

Upon the analysis of the results, we found mainly two types of discrepancy. Firstly, we observe spectral shift of the peak and secondly, a non-spectral uniform difference between the two curves which appears to differ by a linear scaling factor. The former is found to be related to fraction and distribution of clouds in the sky while the latter is determined by the amount of obstruction to the direct solar beam.

As such, the following factor in (22) is suggested, where α and β are empirically determined.

$$E_{\lambda,\mathrm{mod}ified} = \left(\left(\frac{\lambda}{\lambda_{ref}} \right)^{\alpha} + \beta \right) E_{\lambda,measured} \tag{22}$$

4. Results

Figures 15, 17 and 18 below are samples of experimental results of measurement of solar irradiance. Figure 16 shows SMARTS spectrum generated corresponding to figure 15. Over 101 data sets were taken, with 82 global horizontal irradiance measurements and 19 diffuse horizontal irradiance measurements.

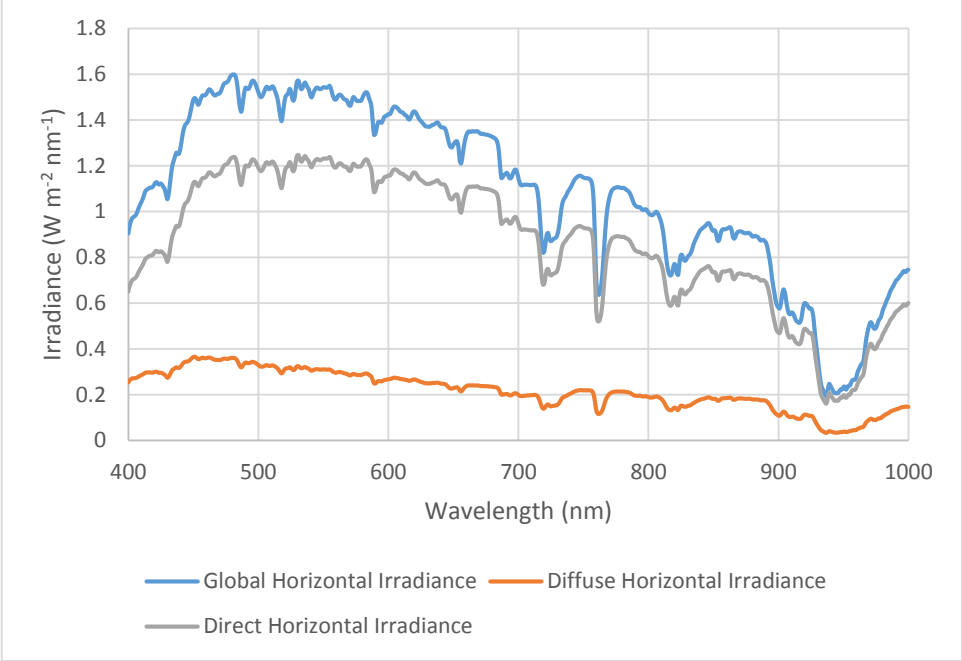

Figure 15 Solar Irradiance measured on a clear sky day with AOD(500nm) = 0.153

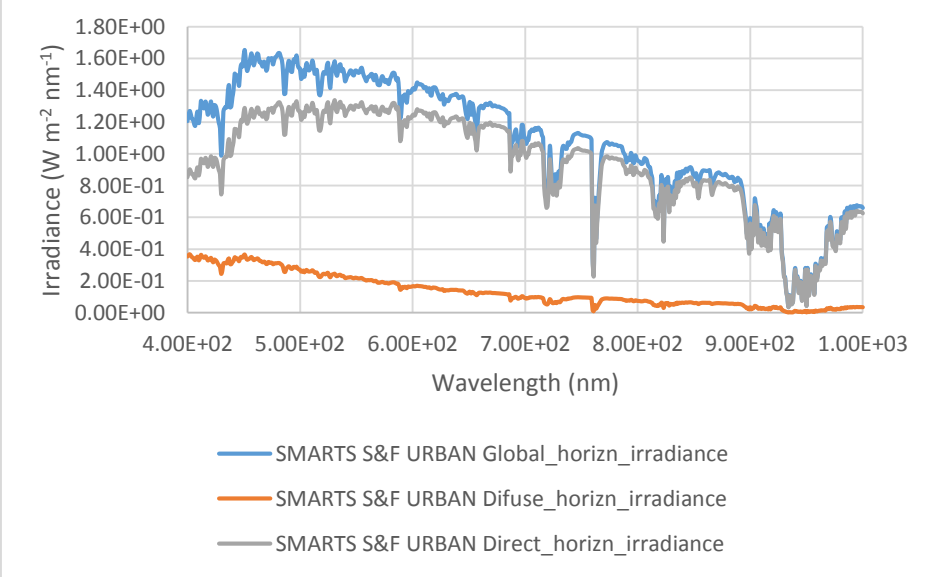

Figure 16 SMARTS Spectrum generated, corresponding to Figure 15

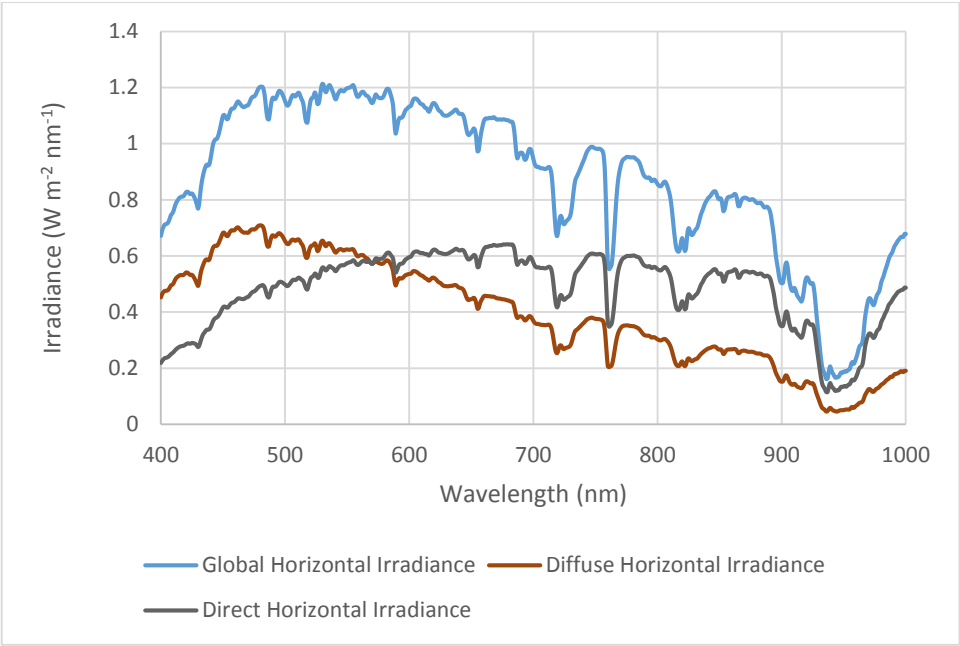

Figure 17 Solar Irradiance measured on a clear sky day with AOD(500nm) = 1.081

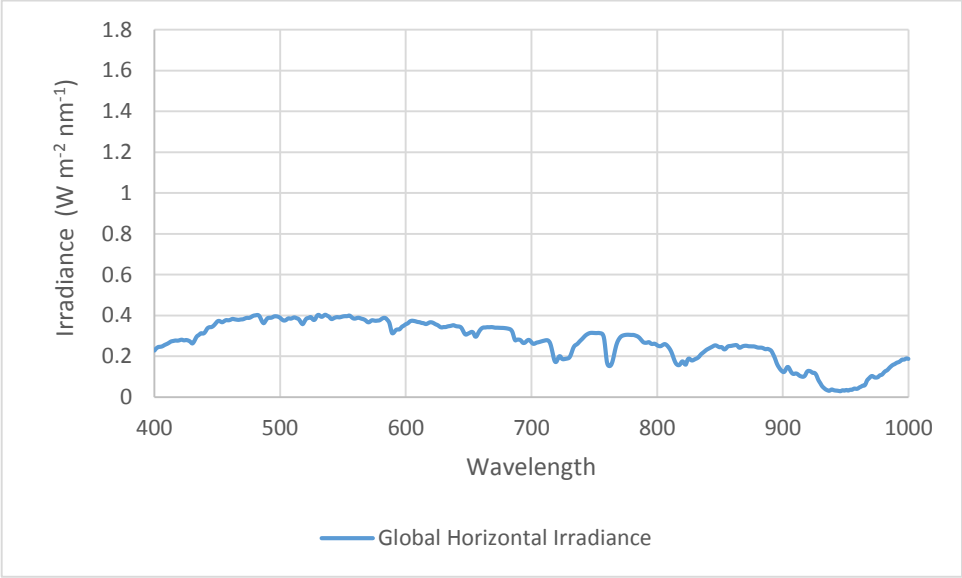

Figure 18 Solar Irradiance measured on an overcast day

5. Data analysis

5.1. Model evaluation

In order to investigate the compatibility between our measured spectrum and the unmodified SMARTS spectrum, we consider the root-mean-square difference (RMSD) between every data point of the two spectrums.

$$RMSD = \sqrt{\frac{\sum_i (x_i - y_i)}{N}} \tag{23}$$

The overall percentage difference, hereafter denoted by ε. between two spectrums is then calculated using (19)

$$\varepsilon = \frac{RMSD}{\bar{x}} \tag{24}$$

Table 1 shows some examples of ε comparison between the SMARTS spectrums and measured data. It also included information of the atmosphere regarding the clouds percentage k, and AOD τ_a(500nm)

Table 1 Sample Table of Data Analysis

#	AOD τ_{a} - (500nm)	Cloud %, k	Was the Sun Disk Obstructed	% difference, ε between measured and SMARTS spectrum ε(400-1000nm) Urban/%	Maritime/%	ε(400-600nm) Urban/%	Maritime/%
1	1.081	4.0	No	10.8	25.4	11.1	29.6
2	1.081	6.0	No	11.6	24.5	11.3	29.3
3	1.081	26.0	Translucent clouds	10.5	47.4	5.66	50.8
4	0.865	26.0	No	10.4	20.3	8.08	25.8
5	0.865	31.0	Translucent clouds	15.7	15.6	14.8	17.2
6	0.153	26.0	No	8.40	8.42	6.43	8.03
7	0.121	12.0	Translucent clouds	8.26	7.91	6.27	7.22
8	0.153	24.0	No	6.96	8.74	6.60	9.86
9	0.153	13.5	No	8.94	8.25	6.49	6.98
10	0.128	20.0	No	8.61	8.71	6.60	8.41
11	0.128	20.5	No	8.47	8.64	6.58	8.56
12	1.081	36.0	Translucent clouds	55.3	109	41.9	104
13	92.18	57.0	Opaque clouds	92.2	158	76.6	154
14	0.128	53.0	Translucent clouds	63.6	63.4	61.6	68.1
15	0.167	99.0	Overcast	160	171		
16	0.167	99.0	Overcast	386	417		…….

5.2 Urban Aerosol Model vs Maritime Aerosol Model

As mentioned in an earlier section, a suitable aerosol model has to be found. Considering only cases where the sky is not overcast for the moment, ε calculated for the entire spectrum from 400nm to 1000nm as follows

Urban Aerosol Model	6.87% - 21.5%
Maritime Aerosol Model	7.84% - 62.4%

It was noticed that the distinction ε between the two models is not great when aerosol optical depth was small. However, when aerosol optical depth becomes larger, ε for maritime model becomes much higher. Figure 19 shows a typical example of this scenario.

Furthermore, the maritime tends to generate a curve which peaks more sharply in the blue-green region, while urban aerosol model gives us a relative flatter spectrum. In this aspect, the urban aerosol model provides a better estimate of the actual measurements. This was reflected in both figure 19 and 20.

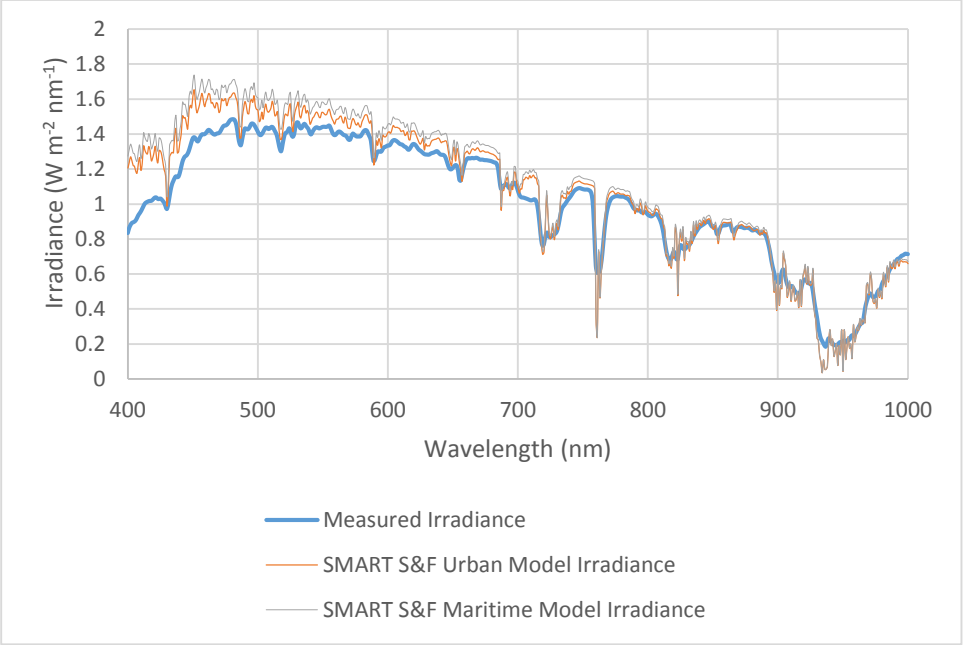

Figure 19 Comparison Between Measures Irradiance, SMARTS Urban Aerosol Model Irradiance and Maritime Aerosol Model irradiance for AOD(550nm) < 1

To assess this fairly, ε is calculated for both spectrum within the range of 400nm to 600nm. Results shows that ε for urban aerosol model range from 5.66% to 24.1% while for maritime models, it ranges from 6.98% to 50.4%

Hence, we could conclude that the urban aerosol model is a more compatible model with the local atmospheric conditions.

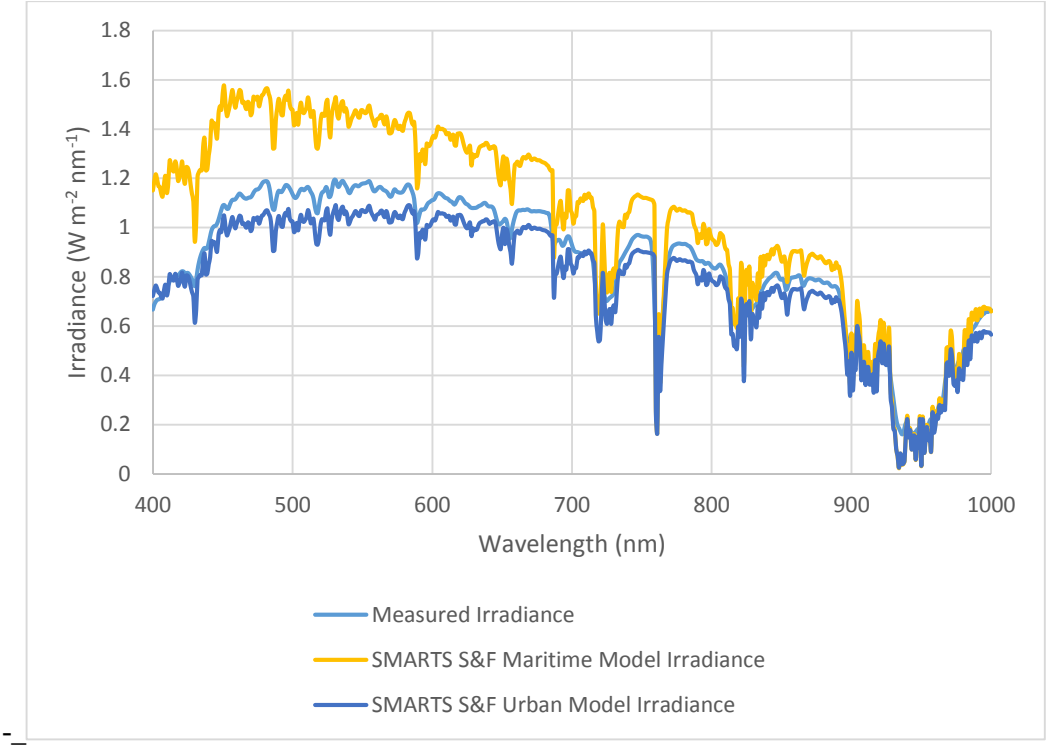

Figure 20 Comparison Between Measures Irradiance, SMARTS Urban Aerosol Model Irradiance and Maritime Aerosol Model irradiance for AOD(550nm) > 1

5.3 Comparison between measured spectrum and unmodified SMARTS spectrum modelled based on S&F urban aerosol model

5.3.1 Compatibility of SMARTS in modelling global horizontal spectral irradiance

In general, under clear or even slightly cloudy sky conditions, SMARTS has shown good compatibility with the measured results. Provided that the sun was not obstructed by thick opaque clouds, ε is found to be less than 20% (6.87% to 18.85%) for datasets with cloud percentage k in the range of 0 to 35%. Given the dynamic environment of the atmospheres, large uncertainties were anticipated. The relatively small RMSD showed good compatibility between the two spectrums. In addition, the data sets within this percentage difference ε

range come from data sets of different atmospheric conditions with some examples shown in table 1.

Thus far, the cases involving overcast skies (k > 90%) have been ignored. This is because SMARTS' ability to predict solar irradiance begins to break down under overcast sky conditions. This incapability extends to situations where the Sun was completely obstructed or when cloud percentage k is high (i.e. when k is greater than 35%). The ε ranges from 51.61% to up to 443.31%. This is expected as the SMARTS model is intended to be a clear sky model and hence, would not be able to deal such situations.

Moreover, in case of overcast skies, the sun disk is not visible. As such, the AERONET sun photometer is not able to provide measurements of the atmospheric content at the time of the overcast sky.

Data sets with intermediate values of clouds percentage has ε in the range of 30.7% to 123.9%.

Since SMARTS is a clear sky model, it can be said that it is rather successful in modelling solar irradiance in the tropical region for clear to slightly cloudy skies.

5.3.2 Compatibility of SMARTS in modelling direct and diffuse horizontal spectral irradiance

RMSD calculations has shown that the compatibility of direct beam irradiance modelling is more so than diffused irradiance. The ε comparing SMART and measured direct irradiance is found to be 4.8% to 37.8% over 19 data sets while the ε percentage for diffuse spectrum was found to be from 7.3% to 86.1%. This result was expect as diffuse irradiance are smaller in value and difficult to model due to its random nature. However, as the number of data sets is

not large. Furthermore, due to the lack proper equipment for measuring direct and diffuse irradiance, the accuracy of the experiment is compromised. Hence, nothing conclusive can be said about the compatibility of SMARTS in modelling direct and diffused component

5.3.3 Source of discrepancies

When analysing the spectrum, main areas of discrepancies happens in the short wave region, as well as overestimates or underestimated of the measured spectrum, as seen in figure 20. The main source of discrepancy between the SMARTS spectrum and experimental results comes from the influence of clouds, which affects the irradiance both spectrally and non-spectrally.

It is also important to consider inherent instrument errors. For instance, the white reflective board is assumed to be Lambertian. However there might be slightly imperfection on the surface which will result in uneven reflection of radiance. Furthermore, the spectroradiometer may also cause inaccuracies due to defects and noise.

Lastly, as seen from the hemispherical photographs, low rise building in the surrounding area occupies about 20% of the sky hemisphere. However, as it lies low on the horizon, its effect on the horizontal irradiance is small.

5.4 Modification of SMART spectrum

5.4.1 Spectral effects of clouds

Counterintuitively, the assumption that clouds will always lead to the flattening of irradiance spectrum does not always agree with the experimental results. This assumption arose because the increase in area of clouds reduces the blue patches in the sky and hence, should reduce the

blue peak of irradiance spectrum. This assumption agrees with our experimental result when aerosol optical thickness is low.

However, our data shows that when aerosol optical thickness is high, the spectrum becomes more peaked in the blue region as compared to clear sky conditions. One possible hypothesis mentioned in *The Spectral Effects Of Clouds (*Bartlett et al.) is that irradiance reflected off the surface clouds causes an increases the amount of scattering. As blue light scatters more, it results in a net increase of diffused blue light reaching the Earth's surface. However, the hypothesis does explain the phenomenon's relation to aerosol optical thickness.

When translucent clouds obstruct the direct sunlight (line of sight), the effects are non-spectral but a decrease in irradiance throughout the entire spectrum

5.4.2 The correction factor

Based on the observations from above, a suitable correction factor suggested by this paper is equation (22) as previously mentioned, where α and β are empirical correction parameters to be determined. Correction parameter α controls the spectral shift while β is a linear scaling factor which scales the irradiance regardless of the wavelength.

$$E_{\lambda,\mathrm{modified}} = \left(\left(\frac{\lambda}{\lambda_{ref}} \right)^{\alpha} + \beta \right) E_{\lambda,measured} \tag{22}$$

The spectral shift factor α is related to cloud factor, with regards to cloud thickness and amount. In case of blue shift, the factor takes a negative value, and conversely, its takes a positive value for red shift or so called flattening of the spectrum.

The linear scaling factor β is intended to be related to the obstruction of sun disk. It is a negative value and it gets more negative as the obstruction of the sun increases. However, upon fitting the training set of data, β was sometimes found to be positive.

Based on the training set of data, we obtain a table of α and β values as follows. By observation, we set λ_{ref} to be 760nm.

From the observation from both tables 2 and 3, with exception of opaque cloud cover of the Sun, β seems to always take a small value of about 0.1. This could be due to some inherent error of the instrument or may be a constant scaling value that relates SMARTS to the actual data. However, this is difficult to determine just based on these numbers as the variation of the β seems random at times. In cases where the Sun is obstructed by thicker clouds, β takes negative values of about -0.2 to -0.4.

As the Sun Disk may get briefly obstructed by faster moving clouds which is impossible to precisely predict the time and duration of occurrence, it is more logical to model β after the cloud percentage, k, value. When k rises above 50% as in table 2, the probability that the Sun Disk will get obstructed is high, hence β will be likely to take negative value at those times.

Table 2 Fitting Parameters obtained by fitting training set with AOD greater than 1

#	AOD τ_a (500nm)	Cloud %, k	Was the Sun Disk Obstructed	Correction Parameters α	β
1	1.081	4.0	No	0	0.1
2	1.081	6.0	Translucent clouds	0	0.1
3	1.081	6.0	No	0	0.1
4	1.081	6.0	No	0	0.1
5	1.081	6.0	Translucent clouds	0	0.1
6	1.081	13.0	Translucent clouds	0	0.1
7	1.081	15.0	Translucent clouds	0	0.2
8	1.081	20.0	Translucent clouds	-0.2	0.2
9	1.081	26.5	Translucent clouds	-0.1	-0.1
10	1.081	36.0	Translucent clouds	-0.2	-0.4
11	1.081	36.0	Near Opaque clouds	-0.2	-0.4
12	1.081	54.0	Near Opaque clouds	-0.15	-0.25
13	1.081	55.0	Near Opaque clouds	-0.15	-0.5
14	1.081	56.0	Near Opaque clouds	-0.15	-0.45
15	1.081	56.0	Near Opaque clouds	-0.1	-0.5
16	1.081	56.0	Near Opaque clouds	-0.1	-0.55
17	1.081	57.0	Near Opaque clouds	-0.1	-0.45

Table 3 Fitting Parameters obtained by fitting training set with AOD greater than 1

#	AOD τ_a(500nm)	Cloud %, k	Was the Sun Disk Obstructed	Correction Parameters α	β
1	0.153	10.0	Translucent clouds	0.1	0.05
2	0.153	12.0	No	0.2	0.1
3	0.153	12.5	No	0.1	0.05
4	0.153	12.5	Translucent clouds	0.15	0.06
5	0.153	13.5	Translucent clouds	0.2	0.1
6	0.153	13.5	Translucent clouds	0.2	0.1
7	0.153	15.0	No	0.2	0.1
8	0.153	15.0	Translucent clouds	0.2	0.08
9	0.128	20.0	No	0.2	0.1
10	0.128	20.5	No	0.1	0.05
11	0.153	22.0	No	0.1	0
12	0.153	24.0	No	0.05	0
13	0.128	25.0	Translucent clouds	0.2	0.2
14	0.128	26.0	No	0.2	0.1
15	0.128	26.0	No	0.2	0.1
16	0.153	29.0	No	0.2	0
17	0.153	32.0	No	0.2	0.1
18	0.153	34.0	No	0.15	0
19	0.128	53.0	Translucent clouds	0.05	-0.35

The behaviour of α on the other hand is dependent on the aerosol optical depth. When aerosol optical depth is greater than 1, trend between α and k can be observed. As k increase to up to 20%, α becomes more negative at about -0.2, that is, the spectrum becomes more peaked in blue region. However, as k continues to rise above 50%, α decrease to about -0.1, that is the spectrum become more flat again. Such trends would seem logical as the percentage of clear sky decreases significantly, the amount blue light reaching the Earth's surface is likely to decrease. In the case where aerosol optical depth is less than 1, α appears to be rather constant, taking values from about 0.1 to 0.2.

Based on the observations from the training set, the following set of values are recommended to fitting any data set provided the knowledge of AOD, and cloud percentage k.

Table 4 Suggested value for correction parameters based on aerosol optical depth and cloud percentage

τ_a>1	k	α	β
	0-20%	0	0.1
	20-30%	-0.2	-0.1
	30-50%	-0.15	-0.4
	>50%	-0.1	-0.4
τ_a<1	<50%	0.15	0.1
	>50%	0.05	-0.4

5.4.3 Compatibility of modified SMARTS

The above suggest correction factor was applied to two sets of testing data as shown in table 5 and 6 respectively. In table 5, with the exception of one case, ε is reduced to less than 10% upon applying the correction. Upon checking the records of case #10 of table 5, it was found that the data was taken when a piece of cloud of over the sun. This was not accounted for in the suggested correction parameters.

The correction for table 6 was not ideal for the cases where k = 25%, where most of the modified SMART spectrum saw an increase in ε. However, for the cases where k = 40%, ε was reduced to about 10% or less in all cases. Upon reviewing the data where k = 25%, such as figure 21, it was found that a more negative α required. This suggest an incomplete understanding at development of fitting parameters.

While the suggested parameters might not work as ideally, the form of the correction factor, equation (22) works rather well, as it is able to address the main discrepancies between the SMARTS irradiance spectrum and the measured spectrum.

Table 5 Testing of modified SMARTS irradiance for AOD at 500nm less than 1

#	AOD τ_{a} (500nm)	Cloud %, k	Suggested Correction Parameters α	β	Percentage RMS Difference: ε Before correction	After correction
1	0.865	31	0.15	0.1	6.87	6.67
2	0.865	31	0.15	0.1	13.4	7.70
3	0.865	31	0.15	0.1	14.2	8.42
4	0.865	31	0.15	0.1	17.7	11.8
5	0.865	31	0.15	0.1	15.7	9.80
6	0.865	31	0.15	0.1	15.9	9.81
7	0.865	29	0.15	0.1	10.8	6.34
8	0.865	29	0.15	0.1	13.7	7.88
9	0.865	29	0.15	0.1	13.5	7.74
10	0.865	29	0.15	0.1	18.7	27.6
11	0.865	29	0.15	0.1	11.1	6.19
12	0.865	26	0.15	0.1	10.4	5.90
13	0.865	25	0.15	0.1	11.8	6.65

Table 6 Testing of modified SMARTS irradiance for AOD at 500nm greater than 1

#	AOD τ_{a} (500nm)	Cloud %, k	Suggested Correction Parameters α	β	Percentage RMS Difference: ε Before correction	After correction
1	1.392	25	-0.2	-0.1	18.1	21.2
2	1.392	25	-0.2	-0.1	19.9	23.2
3	1.392	25	-0.2	-0.1	21.4	24.9
4	1.392	25	-0.2	-0.1	21.5	24.7
5	1.392	25	-0.2	-0.1	27.7	18.6
6	1.392	25	-0.2	-0.1	12.9	7.33
7	1.392	40	-0.15	-0.4	51.6	10.87
8	1.392	40	-0.15	-0.4	66.9	7.88
9	1.392	40	-0.15	-0.4	65.0	7.81
10	1.392	40	-0.15	-0.4	65.4	7.90
11	1.392	40	-0.15	-0.4	73.5	9.82

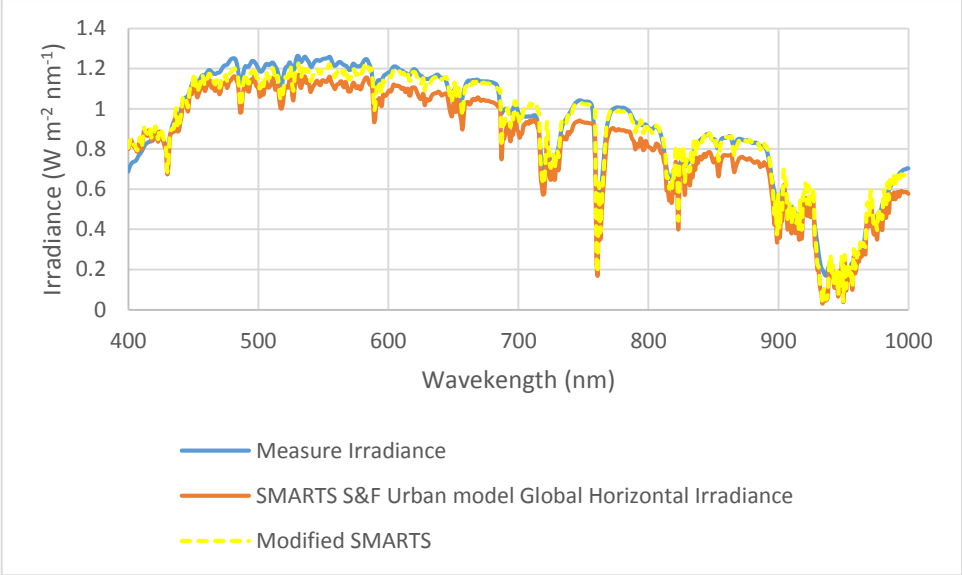

Figure 21 One of the fit SMARTS irradiance curve from table 5

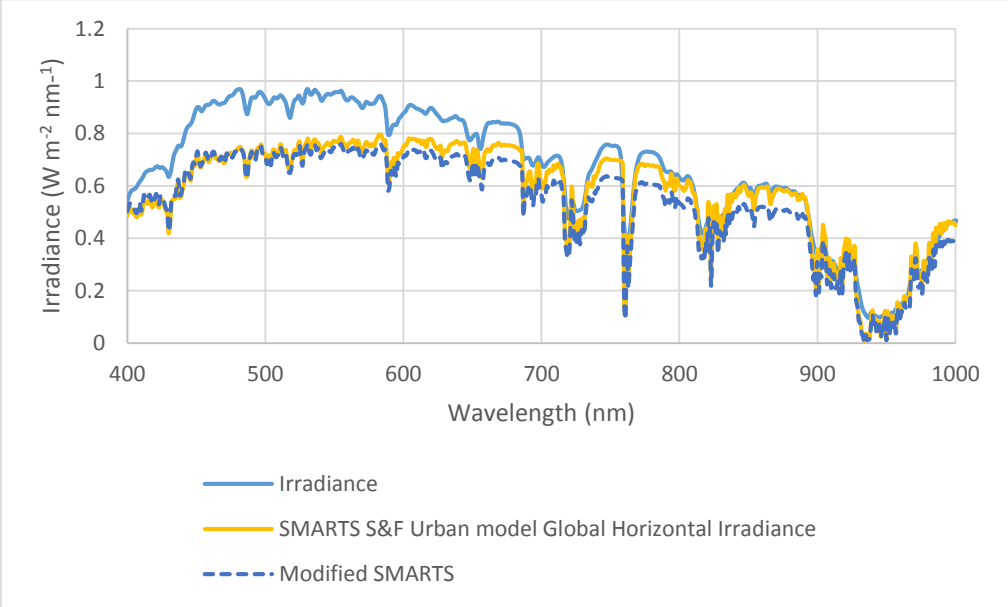

Figure 22 One of the data sets from table 6 where k = 25

5. Conclusion

In conclusion, SMARTS showed excellent compatibility to model local solar spectral irradiance under clear sky conditions or even, under slightly cloudy skies. However, it fails to predict solar irradiance under overcast conditions. While this was expected, overcast irradiance remains an important topic of interest, especially in the tropical regions where humidity is high and rain is frequent. In the development of empirical correction factor, the equation developed was rather simple yet useful as it was able to alter the SMARTS spectrum in the desired manner. However, understanding of the variation of correction parameters α and β require further studies.

References

1 *Shettle, E. P., & Fenn, R. W. (1979). Models for the aerosols of the lower atmosphere and the effects of humidity variations on their optical properties (No. AFGL-TR-79-0214). AIR FORCE GEOPHYSICS LAB HANSCOM AFB MA.*

2 *Gueymard, C. (1995). SMARTS2: a simple model of the atmospheric radiative transfer of sunshine: algorithms and performance assessment. Cocoa, FL: Florida Solar Energy Center.*

3 *Muneer, T. (2007). Solar radiation and daylight models. Routledge*

4 *Gueymard, C. (1995). SMARTS2: a simple model of the atmospheric radiative transfer of sunshine: algorithms and performance assessment. Cocoa, FL: Florida Solar Energy Center.*

5 *Schwalbe, E. (2005, February). Geometric modelling and calibration of fisheye lens camera systems. In Proc. 2nd Panoramic Photogrammetry Workshop, Int. Archives of Photogrammetry and Remote Sensing (Vol. 36, No. Part 5, p. W8).*

6 *NASA Earth Observatory. Clouds and Radiation. (n.d.). Retrieved October 1, 2014, Available from http://earthobservatory.nasa.gov/Features/Clouds/*

7 *Bartlett, J. S., Ciotti, Á. M., Davis, R. F., & Cullen, J. J. (1998). The spectral effects of clouds on solar irradiance. Journal of Geophysical Research: Oceans (1978–2012), 103(C13), 31017-31031.*

8 *Mahdavi, A., & Dervishi, S. (2013). A simple all-weather sky radiance model.IBPSA, Chambery, 916-921.*

9 *Sokoletsky, L., Xianping, Y., & Shen, F. Modeling the Direct to Diffuse Downwelling Irradiance Ratio Based on the Atmospheric Spectral Radiation Model.*

10 *Liang, S., & Lewis, P. (1996). A parametric radiative transfer model for sky radiance distribution. Journal of Quantitative Spectroscopy and Radiative Transfer, 55(2), 181-189.*

11 *Liew, S.C, & Santo, V. (n.d.). AERONET Aerosol Robotic Network. Retrieval of AERONET ground-based Sun-photometer data of Singapore. Last Retrieved March 30, 2015, from http://aeronet.gsfc.nasa.gov/*

12 *Brunger, A. P., & Hooper, F. C. (1993). Anisotropic sky radiance model based on narrow field of view measurements of shortwave radiance. Solar Energy,51(1), 53-64.*

13 *Rosen, M. A., Hooper, F. C., & Brunger, A. P. (1989). The characterization and modelling of the diffuse radiance distribution under partly cloudy skies. Solar Energy, 43(5), 281-290.*

14 *Solar Irradiance Spectrum [Web Drawing]. Retrieved from http://pveducation.org/pvcdrom/properties-of-sunlight/atmospheric-effects*